

# Computation of Damping Derivative of an Ogive at High-Speed Flow

Aysha Shabana\*<sup>†</sup>, Asha Crasta<sup>‡</sup>, Ridwan<sup>‡†</sup>, Sher Afghan Khan<sup>‡†</sup>

<sup>†</sup> Mathematics Dept., M.I.T.E, Moodabidri and Assistant Professor, SCEM, Mangaluru, Karnataka, India

<sup>‡</sup> Mathematics Department, M.I.T.E, Moodabidri, Karnataka, India

<sup>‡†</sup> Department of Mechanical Engineering, Faculty of Engineering, IIUM, Gombak Campus, Kuala Lumpur, Malaysia.

\*Corresponding Author Email: aysha.nawshad@gmail.com

## ABSTRACT

This paper aims to derive an expression for the damping derivative of an ogive in pitch. The Ogive shape is achieved by superposing an arch on the cone. The inertia levels considered are  $M = 5, 7, 9, 10$ , and  $15$ . The contemporary theory applies to the connected shock case & the Mach  $M_2$  behind the shock  $M_2 \geq 2.5$ . Damping derivatives are examined for ogive for  $\gamma = 1.4$  at various semi angles for differing pivot positions and Mach numbers and  $\lambda = \pm 5, 10$ . Results indicate a continued decrease in stability derivatives. However, the damping derivatives turn independent of Mach  $M$  for Mach more than ten— with a surge in the cone angle, a continued rise in the damping derivatives attained.

## KEYWORDS

high-speed flow, damping derivative, delta wing, ogive

## INTRODUCTION

There have been rapid developments in supersonic/hypersonic flow recently with the advent of supersonic/hypersonic missiles and aerospace vehicles. There is a need to develop a theory to compute the stability derivatives at these high speeds. In the absence of wind tunnel results, analytical computation of the stability derivatives serves as an efficient tool to optimize the design of the missiles and aircraft to reduce the number of experiments and costs. The present work aims to derive the expression for ogive at hypersonic Mach numbers. The Ogive shape is achieved by superposing an arch of  $\lambda = \pm 5, \pm 10$  for the cone surface. The ogival shape of the nose has numerous advantages over the conical nose shape. A single powerful shock wave for the entire nose length of the cone, and its strength will remain constant for the whole dimension of the nose. Whereas, in the case of the ogival nose shape, there is a continuous slope change; hence, all along the length of the nose resulting in Mach waves where the entropy of the flow will remain unchanged and will negligible loss in pressure energy. The ogive's packaging efficacy is maximum compared to a conical nose. It increases the payload capacity of aerospace vehicles. Ghosh, K., [1] devised another hypersonic similitude for the attached shock case. The Mach after the shock must be more than 2.5 (i.e.,  $M_2 > 2.5$ ). He ignored the impact of the Lee surface as the contribution from the Lee surface was negligible. He mainly focussed on the side accompanied by an oblique shock wave at the plate.

They further stretched his work for cones and delta wings by Ghosh [1,2]. Khan and Crasta [3], Crasta et al. [4,5], Aysha et al., [6-8] used Ghosh's theory of [1] and [2] to supersonic/hypersonic delta wings and cones. Renita et al. [9] study the effect of secondary wave reflections on wings at supersonic/hypersonic flow. Renita et al. [10] did a comparative study of quasi-steady and unsteady and computed stability derivatives for wings with curved leading edges. Wings with edges having curvature has some distinct benefits over straight leading edges. When the wing's leading edge is curved by superposing a half-sine wave, the wing area shifts significantly towards the trailing edge— owing to the change over of the wing area downstream, resulting in a substantial rise in the stability derivatives of the

aerospace vehicles. Interestingly, the study of high-speed flow was limited to a slim body, and small angles of incidence are extended for high angles of attack. Khan et al. [11,12] studied using CFD to compute the flow around the two-dimensional wedge. Additionally, some studies has found that related to current work in which different theories was used to study the stability of delta wing [13-15].

## METHODOLOGY

From Figure 1, we get

$$\tan \phi = \frac{x \tan \theta}{(x - x_0)} ; \tan \phi_0 = \frac{c \tan \theta}{(c - x_0)}$$

Where  $\phi$  is the angle delimited by point A at  $O'$  with x-axis,  $\phi$  varies from  $\pi$  to  $\phi_c$ ,  
 $\theta_c + \lambda =$  cone angle, and  $c =$  chord size.

The characterization of the Stiffness coefficient symbolized through  $C_{m_\alpha}$

$$C_{m_\alpha} = \left[ \frac{\partial M}{\partial \alpha} \right]_{\alpha, q \rightarrow 0} \frac{1}{\frac{1}{2} \rho_\infty U_\infty^2 S_b c}$$

$$S_b = \text{ogive cross-sectional area} = \pi (c \tan \theta_c)^2,$$

$c =$  chord size.

On resolving, we get,

The expression for cone zero angles of incidence and pressure ratio after and before shock [2], with the connected shock with an ogive nose

$$\frac{P_{bo}}{P_\infty} = 1 + \gamma M_{po}^2 \left( 1 + \frac{1}{4} \varepsilon \right) \quad (1)$$

Density ratio is

$$\varepsilon = \frac{2 + (\gamma - 1) M_{po}^2}{2 + (\gamma + 1) M_{po}^2} \quad (2)$$

$M_{po} =$  piston Mach, operating in a conical-annular area;  $P_{bo} =$  ogive surface pressure.

$$M_{po} = M_\infty \sin \theta_c$$

$\theta_c =$  ogive angle

Hence

$$\frac{dP_{bo}}{dM_{po}} = 2\gamma P_\infty M_{po} \left[ 1 + \frac{1}{4} \left( \varepsilon + \frac{1}{2} M_{po} \cdot \frac{d\varepsilon}{dM_{po}} \right) \right] \quad (3)$$

Where

$$\frac{d\varepsilon}{dM_{po}} = \frac{-8M_{po}}{N^2} + \lambda' f \left\{ \frac{8K(3(\gamma+1)K^2 - 2)}{N^3} \right\} \quad (4)$$

$$\& N = [2 + (\gamma+1)M_{po}^2]$$

On solving (3), we get

$$\frac{dP_{bo}}{dM_{po}} = 2\gamma P_{\infty} M_{po} \left[ (a_1 + \lambda' a_2) - \frac{2a_2 \lambda' h \tan \phi}{\tan \phi - \tan \theta_c} \right] \quad (5)$$

$$h = \frac{x_0}{c},$$

$$\lambda' = \frac{\lambda}{\tan \theta_c},$$

$$a_1 = 1 + \frac{\varepsilon}{4} - \frac{K^2}{N^2}$$

$$\text{And } a_2 = 1 + \frac{\varepsilon}{4} - \frac{K^2(N+8)}{N^3}$$

The formulae for Stiffness and damping derivative is obtained from the above

$$C_{mq} = [C_{mq}]_{cone} + \frac{\lambda' a_2}{15(1+n^2)} \left[ h^4 \{5(2n^2 - 3n^4 - 1) - 4h(3n^2 - 6n^4 - 1)\} + (1-h) \{H(9H + (2n^2 - 3H)h) + 2(2H + 3n^2)h^2 + 12n^2 h^3\} - n^4 h^2 (1 + 3h - 24h^2) \right]$$

Where

$$[C_{mq}]_{cone} = (D/2) \left[ h^4 (2n^2 - 3n^4 - 1) - (1-h) \{H(3H + h(H + 2n^2) + 2h^2 n^2) + n^4 h^2 (1 + 3h)\} \right]$$

$$D = \frac{2}{3(1+n^2)} \left[ 1 + \frac{1}{4} \left( \varepsilon + \frac{1}{2} K \frac{d\varepsilon}{dM_{po}} \right) \right]$$

$$H = (1 - h + n^2)$$

$$\text{And } n = \tan \theta_c$$

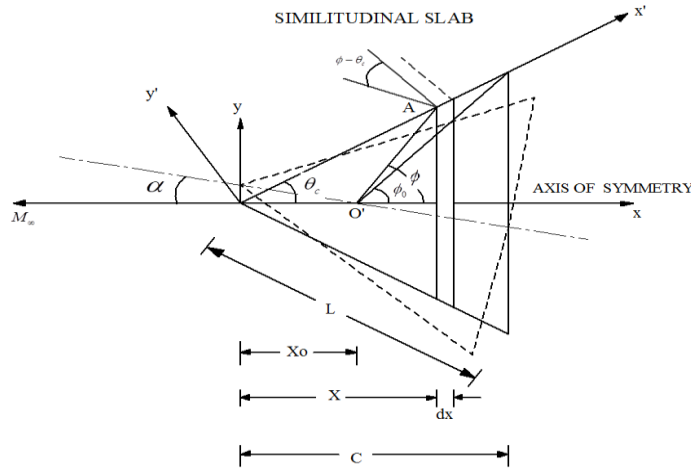


Figure 1. Geometry

RESULTS AND DISCUSSIONS

The expressions derived from the previous section generated data for damping derivatives in pitch. The results are plotted by varying Mach number, flow deflection angles, for different ogive arch, against the pivot parameter  $h$ .

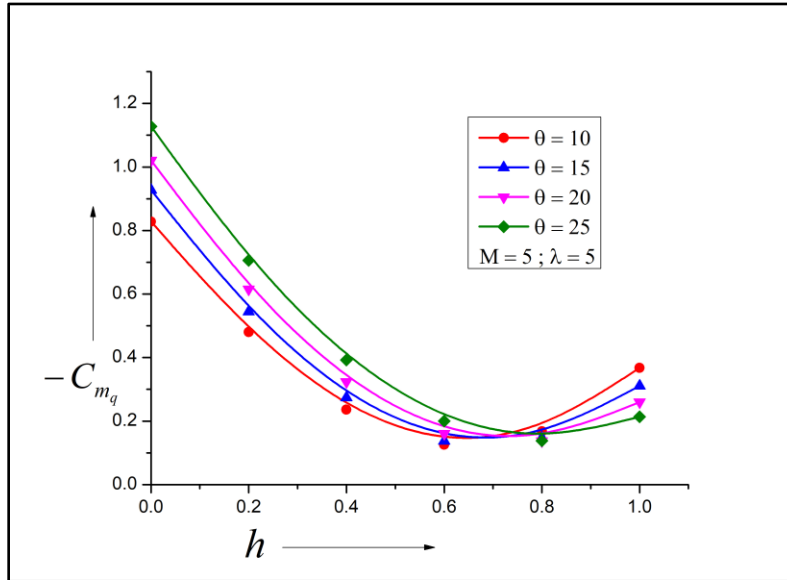


Figure 2.  $C_{mq}$  Vs.  $h$ ,  $M = 5$ ,  $\lambda = 5$

At the lowest Mach number of the present study (i.e.,  $M = 5$ ), the study's findings are presented in Figure 2 for cone angles  $10^\circ$  to  $25^\circ$  and the ogive arch  $\lambda = 5$ , at different pivot locations. It is realized that there is a rise in  $C_{mq}$  as the cone angle increases. This rise in the cone angles raises the wetted area of the ogive, and hence the growth is quite natural. Results also show a gradual decrease in damping as we move towards the trailing edge. A reversal in the trends occurs at  $h = 0.72$ , and reversal of the variable is ascribed to the pivot point's location and variation in surface pressure. The minima point of the damping derivatives moves downstream when the cone angle rises from 10 to 25 degrees.

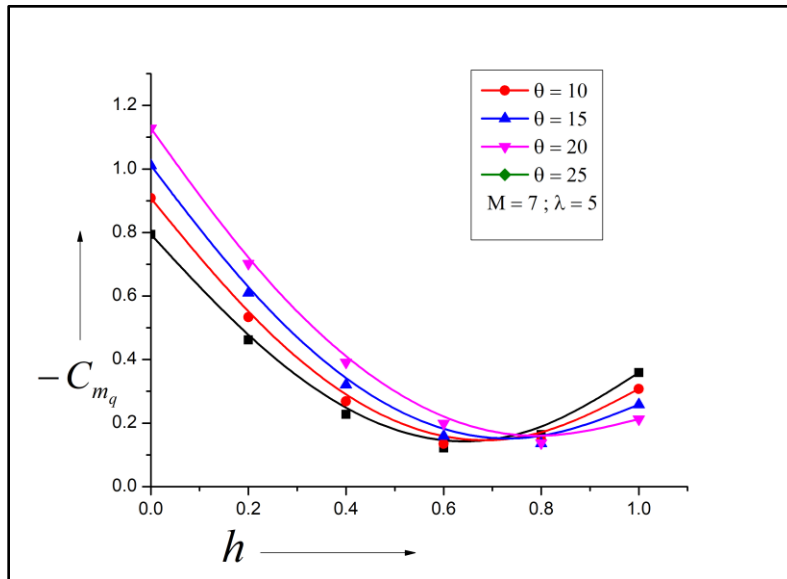


Figure 3.  $C_{mq}$  Vs.  $h$ ,  $M = 7$ ,  $\lambda = 5$

Figure 3 shows outcomes of the study for a case where Mach is marginally enhanced to  $M = 7$  from 5, keeping all the geometrical variables the same. The results show a negligible reduction in the amplitude of  $C_{mq}$  with an increase in the inertia levels. The decrease in  $C_{mq}$  is ascribed to the change of pressure intensity and its spreading on the surface of ogive. The reversal remained almost at the same point as at Mach  $M = 5$ . The minima point of stability derivatives remains unchanged due to a negligible rise in inertia levels and hence the pressure intensity over the ogive surface.

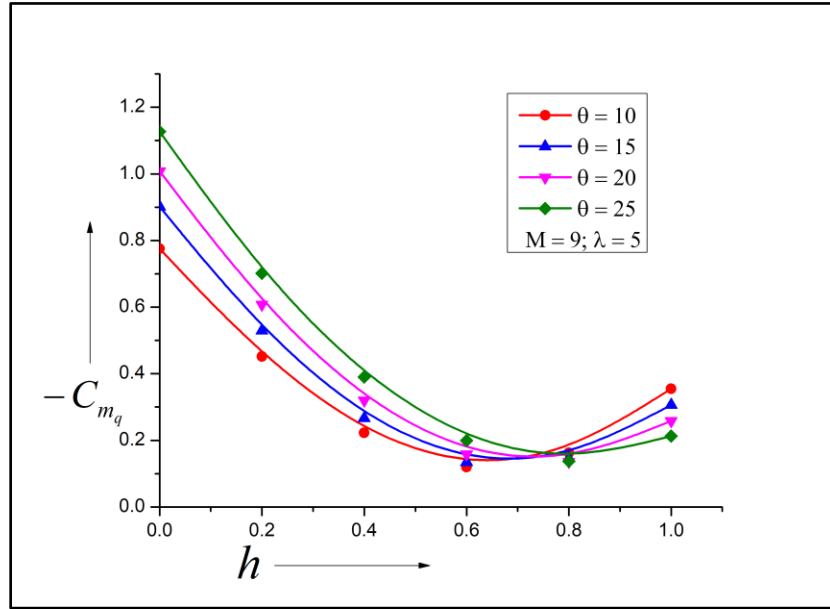


Figure 4.  $C_{mq}$  Vs.  $h$ ,  $M = 9$ ,  $\lambda = 5$

An escalation of Mach from  $M = 7$  to 9 shows similar outcomes in Figure 4 for the damping derivatives and reiterates that there will be a marginal decline in the damping derivatives. A minimal decrease in the value of  $C_{mq}$  is due to the rise in Mach values. Since the cone angles remained unchanged, the position of the normal force remained unchanged. In all these results, the magnitude of  $C_{mq}$  is at a peak for  $h = 0$ . Later downstream, there is a gradual decrease in their numerical values as the pitching point is shifted towards the trailing edge.

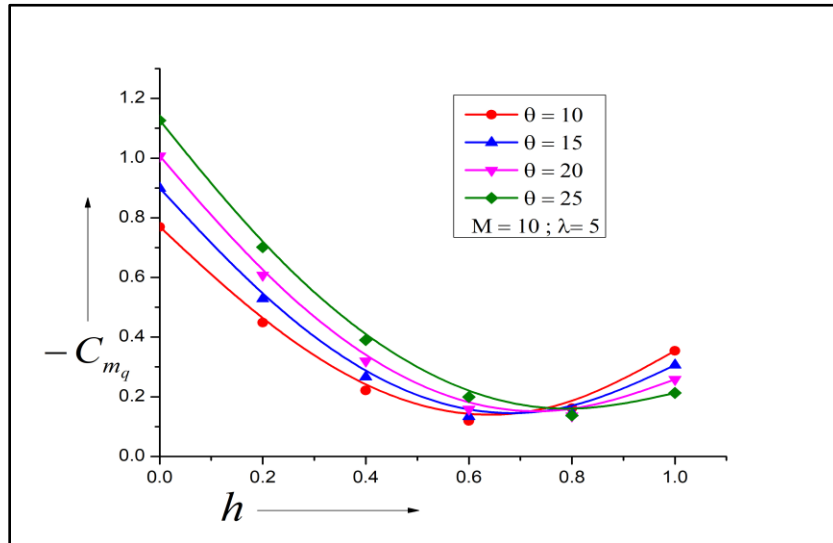


Figure 5.  $C_{mq}$  Vs.  $h$ ,  $M = 10$ ,  $\lambda = 5$

When Mach  $M = 10$ , the damping derivative in pitch is shown in Figure 5, holding all other geometrical constraints the same, inertia level  $M$  has risen  $M = 9$  to  $10$ , and outcomes reveal no augmentation in the numerical values of the stability derivatives at this Mach. An ongoing decline in the value of the damping derivatives with an increase of Mach numbers has vanished. This tendency can be attributed to the circumstance that when the Mach is raised to a specific threshold value, there may be no variations in the  $C_{mq}$ . Once this steady state is achieved in the stability derivatives, flow variables become independent of the Mach number, and we say that Mach number independence has occurred

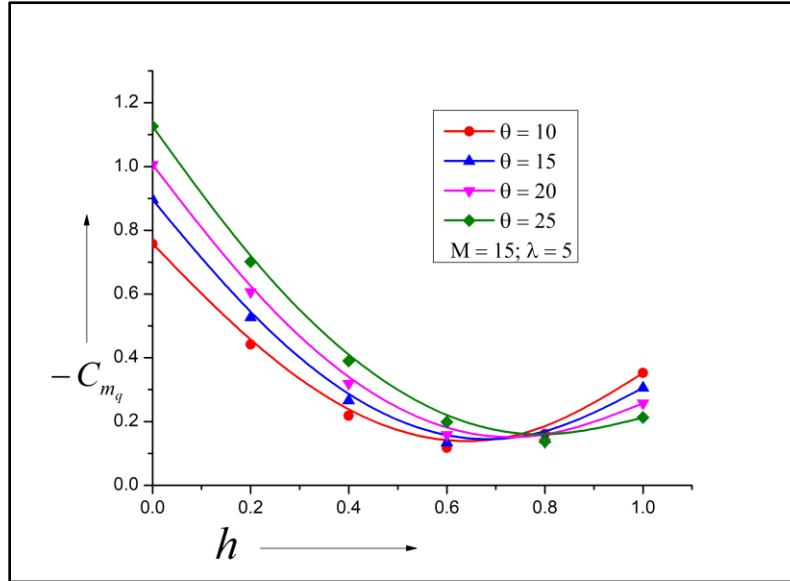


Figure 6.  $C_{mq}$  Vs.  $h$ ,  $M = 15$ ,  $\lambda = 5$

At the highest Mach number at  $M = 15$ , it is seen that there is no variation of  $C_{mq}$  at this Mach. The Mach numbers independence principle holds, which has already been achieved for Mach ten. Hence the stability derivatives remain constant along with all its properties.

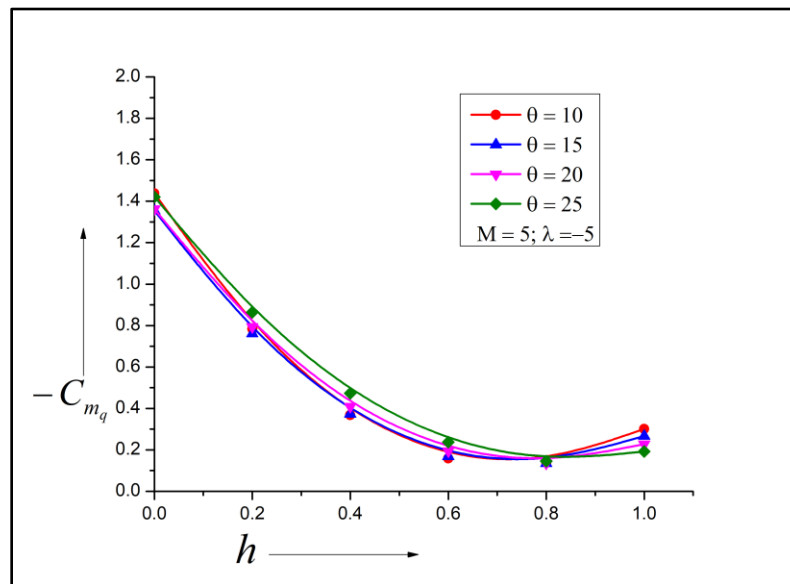
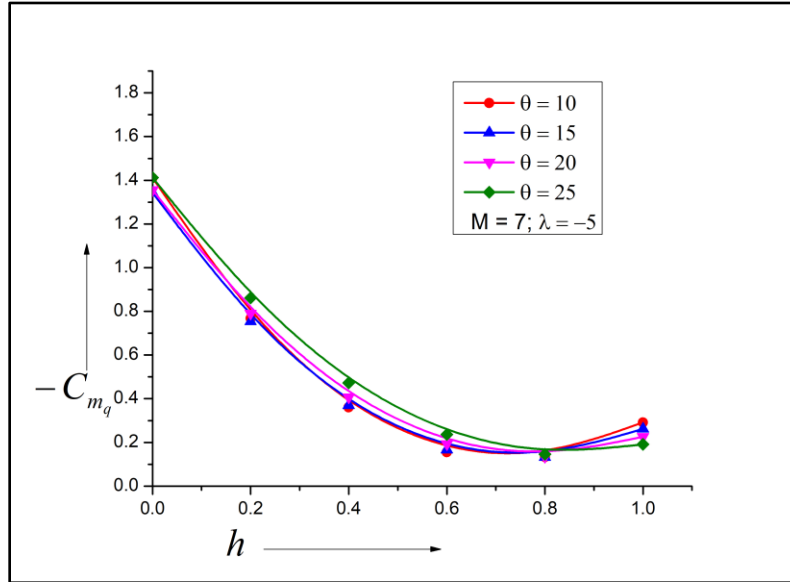


Figure 7.  $C_{mq}$  Vs.  $h$ ,  $M = 5$ ,  $\lambda = -5$

So far, the arch was either  $\lambda= 5$  or  $10$ , now, the upcoming damping derivatives results are for  $\lambda= -5$  or  $-10$  for the same range of inertia values, and geometrical parameters are shown in Fig.3 to 6. For  $\lambda= -5$ , a marginal rise in  $C_{mq}$  when cone angles range from  $10$  to  $20$  degrees. An overall growth in  $C_{mq}$  for all theta values. However, a significant surge in  $C_{mq}$  is observed for cone angle equals twenty-five degrees. It may be due to the cone shape changes because of growth in the cone surface area. The trend reversal is shifted downstream at  $h = 0.8$  for cone angle twenty-five degrees. However, the minima of  $C_{mq}$  remained in the range from  $h = 0.7$  to  $0.8$ . That shows that the aerospace vehicle will be more dynamically stable at the highest angle of twenty-five degrees.



**Figure 8.**  $C_{mq}$  Vs.  $h$ ,  $M = 7$ ,  $\lambda = -5$

When Mach  $M = 7$ ,  $C_{mq}$  Vs. Pivot position  $h$  is shown in Figure 8, and all other parameters are unchanged. Similar results are seen at Mach  $M = 7$  with a marginal decline in the damping derivatives' values due to the growth of inertia levels. Once again, it is observed that the numerical values of  $C_{mq}$  remained nearly the same, and any rise in the cone angles does not show a significant change in the damping derivatives. However, when the cone angles are twenty and twenty-five degrees, it offers some fluctuations in  $C_{mq}$  owing to a considerable increase in the surface area. The minima have been shifted marginally in the direction of the flow. Alteration in the least of  $C_{mq}$  may be one of the positive at this Mach  $M = 7$ . Consequently, a change in the center of pressure will yield the most superior and effective results in aerospace vehicles' static and dynamic stability.

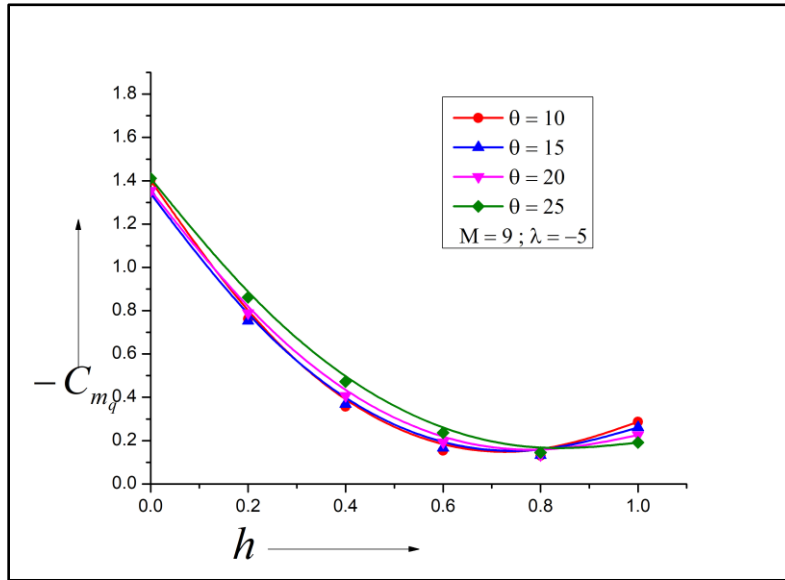


Figure 9.  $C_{mq}$  h,  $M = 9$ ,  $\lambda = -5$

Here Mach is raised from  $M = 7$  to  $9$ , variations in the stability derivatives are presented in Figure 9 for cone angles from  $10$  to  $25$  degrees and  $\lambda = -5$ . A minimal reduction in the magnitude of  $C_{mq}$  when the inertia is high. A reversal in the trend remained around  $h = 0.8$  at a single point. Owing to a rise of Mach from  $M = 7$  to  $9$ , this trend was expected as the inertia level has nearly reached a value that is likely to convert steady and self-regulating of Mach. As the center of pressure remained around  $h = 0.8$ , this configuration will continue to stay dynamically stable despite having smaller values of  $C_{mq}$ . Under these circumstances, the movement of the center of pressure is more prominent and yields larger values of damping derivatives, and can quickly compensate for a marginal decline in the damping derivatives.

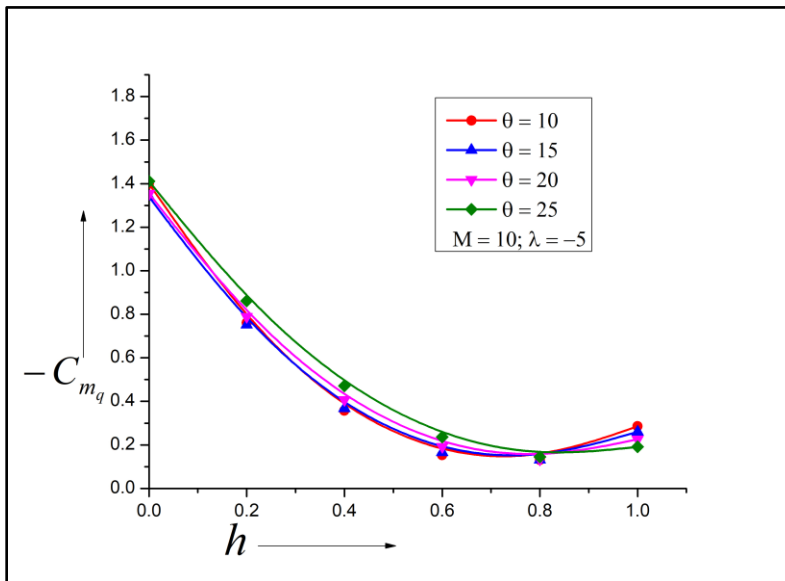


Figure 10.  $C_{mq}$  Vs. h,  $M = 10$ ,  $\lambda = -5$

When Mach  $M = 10$ , Figure 10 displays the findings of stability derivatives for various cone angles from ten to twenty-five degrees. Results show no change in the numerical values as the Mach number independent principle will hold at these Mach numbers. Once again, there is an appreciable change in the stability derivatives for cone angle  $25$  degrees.

From these results, we may say that one angle of 10 to 20 degrees is not desirable for the given parameters and should not be considered to finalize the dimensions of the aerospace vehicles. It is also realized that constant values of  $C_{mq}$  will not hamper the mission requirement. The center of pressure has shifted downstream, resulting in a substantial increase in the moment arm for  $C_{mq}$ , and the system becomes dynamically stable.

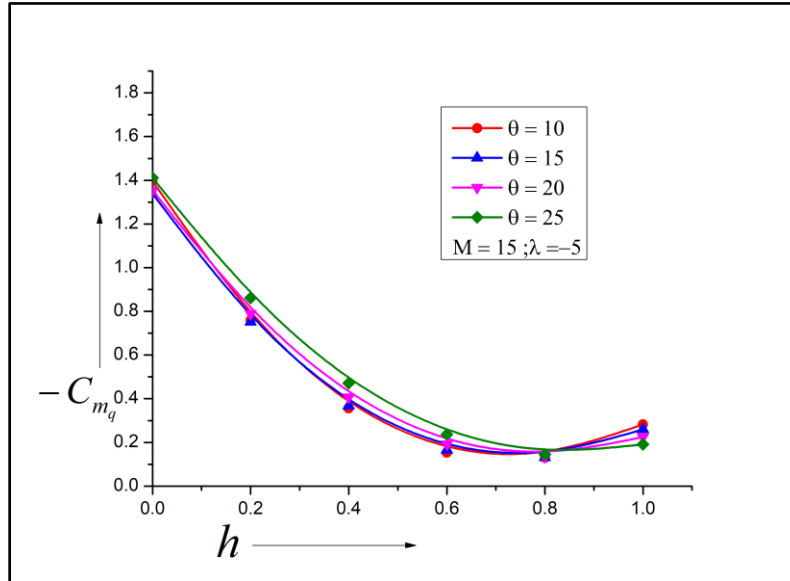


Figure 11.  $C_{mq}$  Vs.  $h$ ,  $M = 15$ ,  $\lambda = -5$

Figure 11 shows results for the peak Mach  $M = 15$  at  $\lambda = -5$ ; as discussed earlier, aerodynamic derivatives have become independent of Mach number due to the Mach number autonomous condition. At this Mach, a marginal change in the center of pressure will be beneficial from the dynamic stability considerations.

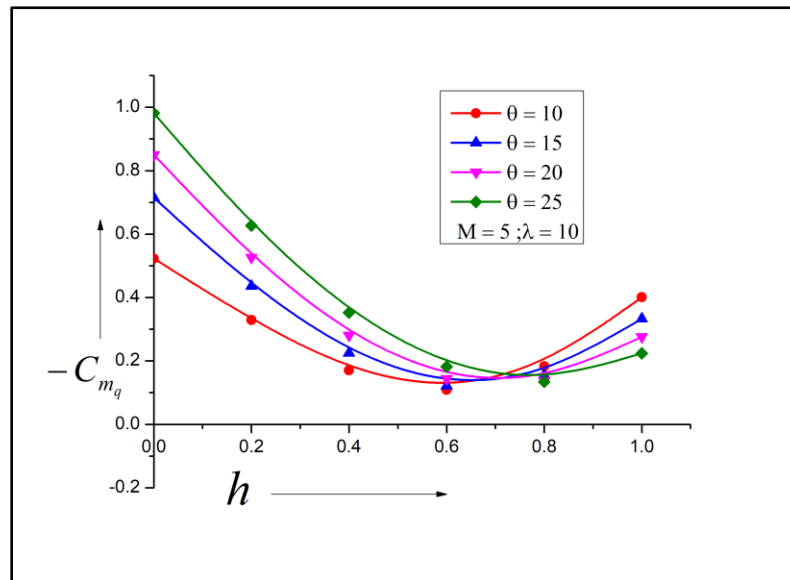


Figure 12.  $C_{mq}$  Vs.  $h$ ,  $M = 5$ ,  $\lambda = 10$

Figure 12 demonstrates a variation of  $C_{mq}$  Vs. non-dimensional pivot position  $h$  for Mach 5 and the most significant value of  $\lambda = 10$ . Because of the increase in the  $\lambda$  value, there is a substantial change in the shape and surface area of the ogive, significantly reducing the damping derivatives. The reversal in the pattern varies from  $h = 0.65$  to  $0.8$ . This

change in the reversal pattern is because of the shape change in the nose part of the cone. The outcomes show that even though a decline in the numerical value of the damping derivatives is seen. However, the contribution from the movement of the center of pressure is significant. The shift of pressure location will compensate for the losses incurred in the damping derivative. Finally, the aerospace vehicle remains dynamically stable.

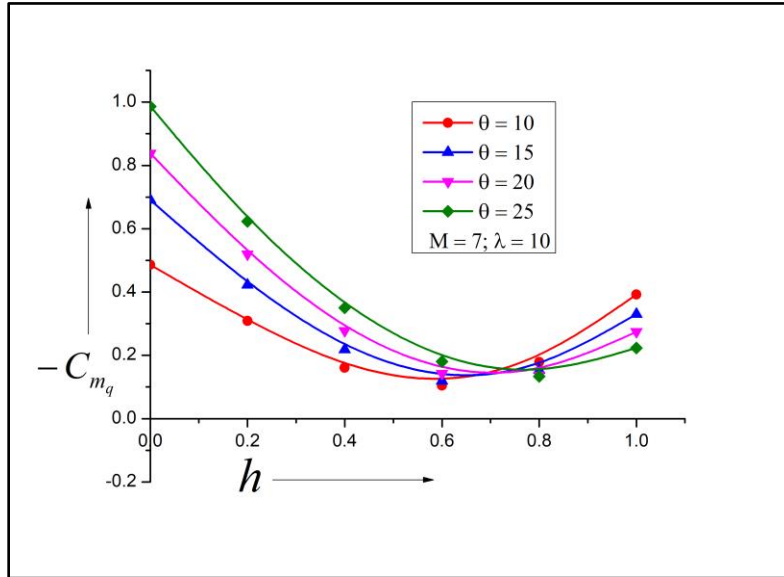


Figure 13.  $C_{mq}$  Vs.  $h$ ,  $M = 7$ ,  $\lambda = 10$

Outcomes of the present study when Mach  $M = 7$  are presented in Figure 13, where all other variables remained similar except that the inertia level has augmented from  $M = 5$  to 7. Due to an increase of Mach, there is a minimal decline in the damping derivatives. There is a marginal swing in the reversal pattern in the values towards the downstream. This rise in the value of the control reversal will enhance the pitching moment magnitude and render the system dynamically stable.

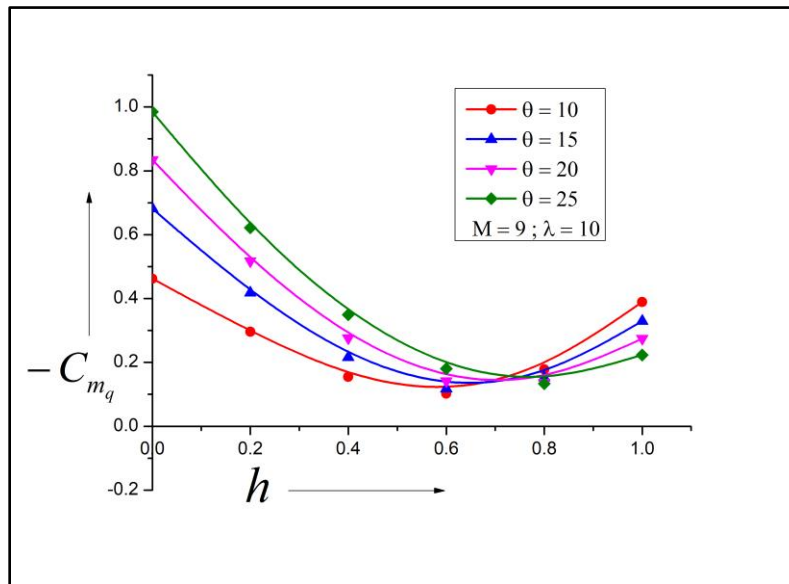
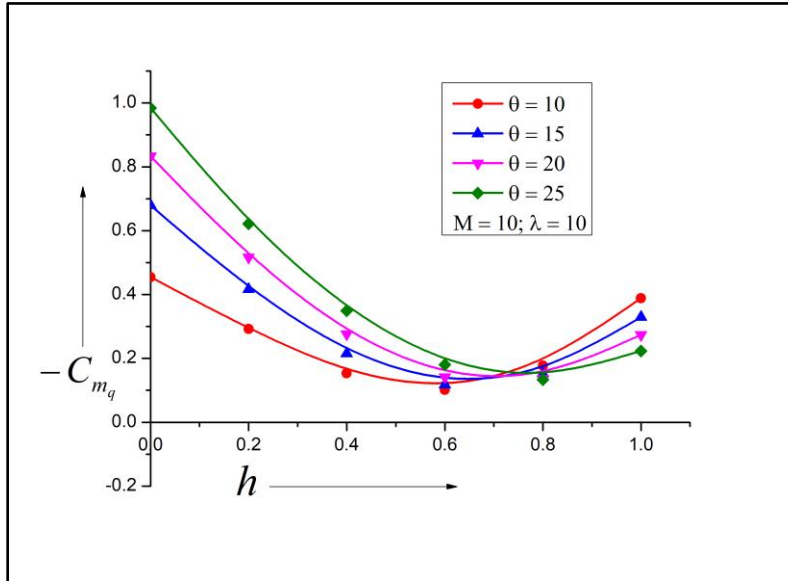


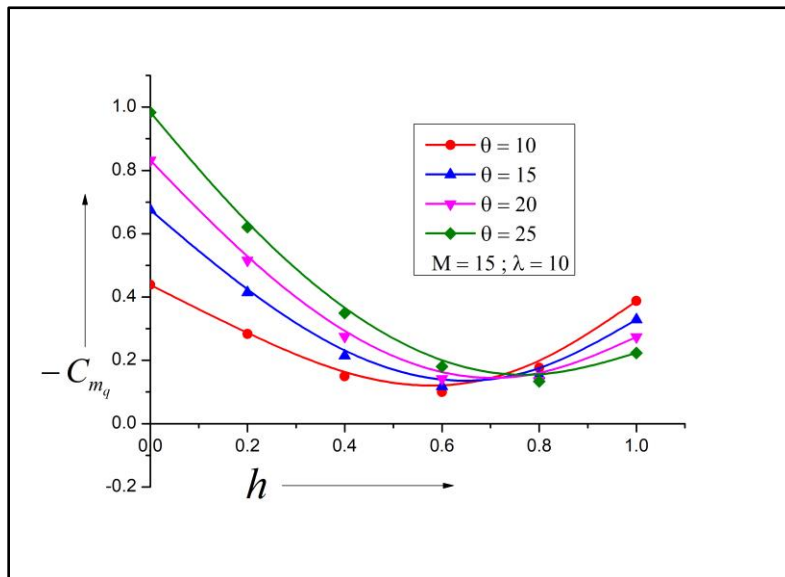
Figure 14.  $C_{mq}$  Vs.  $h$ ,  $M = 9$ ,  $\lambda = 10$

At Mach  $M = 9$ , the outcomes of the present study are shown in Fig. 14. Meanwhile, the Mach has risen from 7 to 9, the stability derivatives have further decreased. The band of the pattern reversal, which was very large, is getting narrowed down and is limited between  $h = 0.65$  to  $0.75$ . A progressive rise of  $C_{mq}$  is due to the surge of cone angles. This increase remained maximum for the pivot position  $h = 0$ . The damping derivatives' magnitude also declines when the pivot point moves downstream.



**Figure 15.**  $C_{mq}$  Vs.  $h$ ,  $M = 10$ ,  $\lambda = 10$

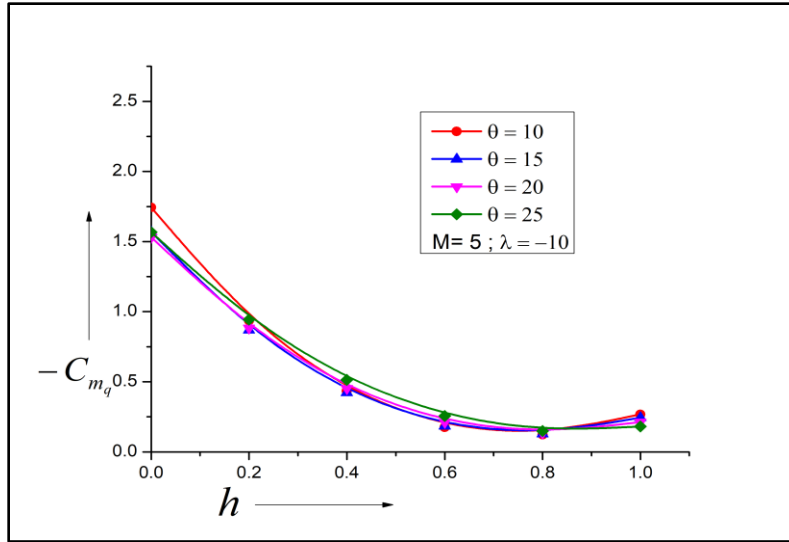
Similar results are seen in Figure 15 when Mach number  $M = 10$ ; however, their numerical values are nearly constant as the Mach number is appreciably high. Any escalation of Mach does not influence the magnitude of  $C_{mq}$ . The causes for this tendency are the same as discussed before.



**Figure 16.**  $C_{mq}$  Vs.  $h$ ,  $M = 15$ ,  $\lambda = 10$

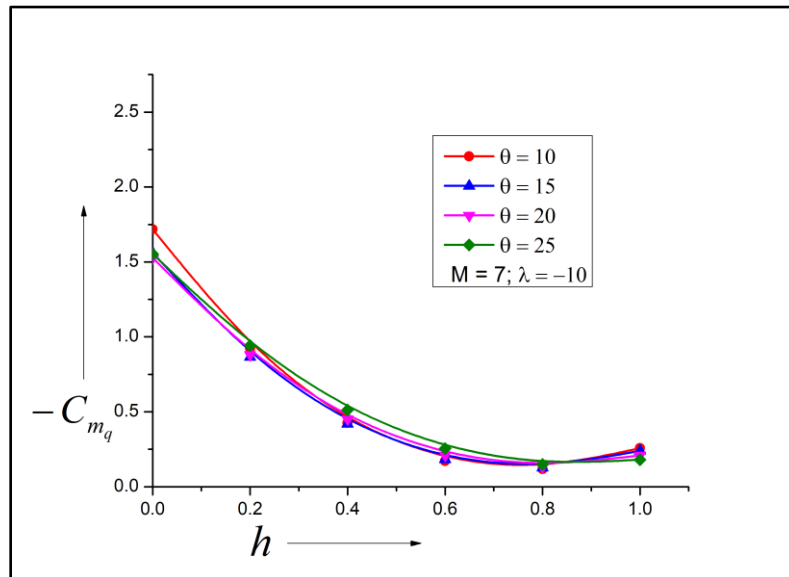
At the Mach number of the present study  $M = 15$ , variation in the damping derivatives is shown in Figure 16 at  $\lambda = 10$  for different cone angles. Since inertia levels are high, any boost in the Mach  $M$  will not influence the damping

derivatives' magnitude because of the independence principle. There is a marginal swing in the position of the resultant force, which will be helpful when the dynamic stability is computed.



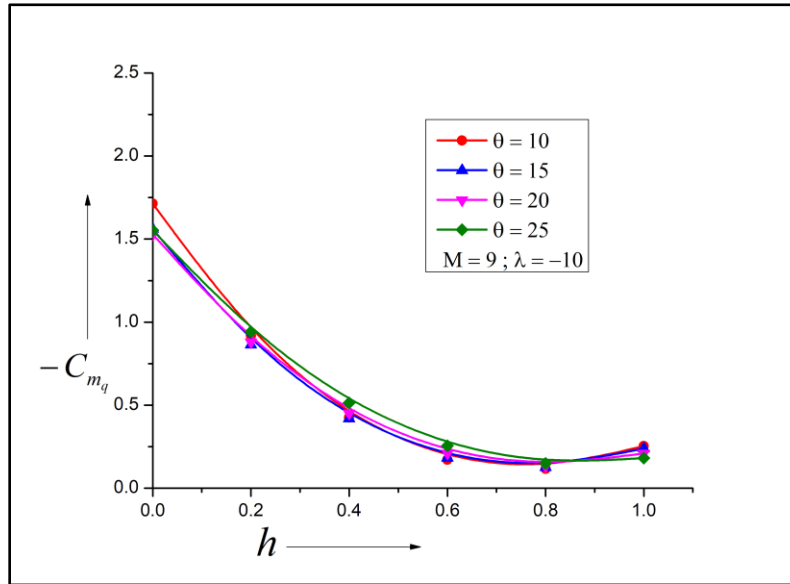
**Figure 17.**  $C_{mq}$  Vs.  $h$ ,  $M = 5$ ,  $\lambda = -10$

Figure 17 displays variations in the damping derivatives with various pivot positions at different cone angles when  $\lambda = -10$ . For this shape of the ogive, there is no definite pattern seen. Within  $h = 0$  to  $0.2$ , damping derivative takes higher values for cone angle = 10 degrees, later in the downstream of the cone from  $h = 0.3$  till  $0.8$  damping derivatives assumes marginally higher values and reversal in the trends takes place at  $h = 0.85$ . Based on the above observation, this design may suit a single cone angle and not like other cases where the damping derivatives increase with the increase in the cone. The physics of this pattern can be understood when we do numerical simulations of the flow using a suitable turbulence model.



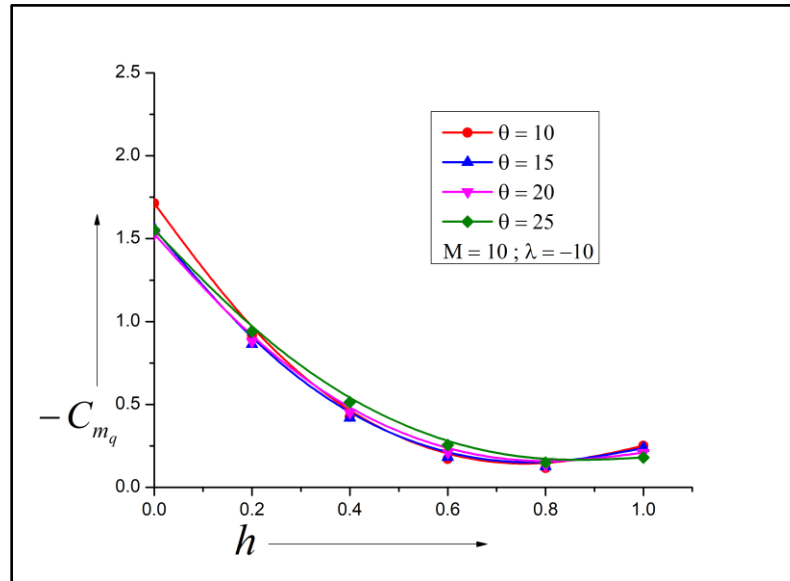
**Figure 18.**  $C_{mq}$  Vs.  $h$ ,  $M = 7$ ,  $\lambda = -10$

Figure 18 shows similar results for an increased Mach  $M = 7$ . The figure shows a marginal decrement in the stability derivatives, and behavior shows a similar pattern as in the previous case for Mach  $M = 5$  in Figure 17.



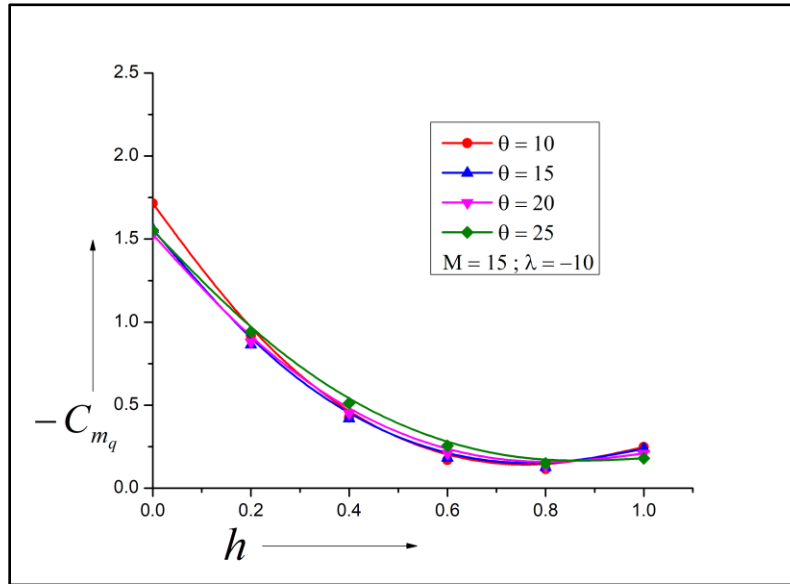
**Figure 19.**  $C_{mq}$  Vs.  $h$ ,  $M = 9$ ,  $\lambda = -10$

Figure 19 shows similar results for Mach  $M = 9$  as seen in the previous two Mach numbers, namely  $M = 5$  and  $7$ . As the Mach number has increased considerably, any surge in Mach  $M$  will not generate any variation in the damping derivatives as the flow has reached a limiting level. All parameters will remain constant despite an increase in the inertia levels. The effect of cone angles also reveals similar trends, as was seen at smaller Mach  $M$ .



**Figure 20.**  $C_{mq}$  Vs.  $h$ ,  $M = 10$ ,  $\lambda = -10$

Findings at Mach  $M = 10$  are displayed in Figure 20, without changing all other parameters. Due to the high Mach number, we do not observe the impact of the growth of Mach on the magnitude of  $C_{mq}$  as the damping derivative has achieved a steady state.



**Figure 21.**  $C_{mq}$  Vs.  $h$ ,  $M = 15$ ,  $\lambda = -10$

Figure 21 displays the variation of  $C_{mq}$  pivot Vs.  $h$  at Mach  $M = 15$ , and  $\lambda = -10$  for cone angle from 10 degrees to 25 degrees. As discussed earlier, these combinations of the parameters are not helpful as marginal changes in the damping derivatives are observed. There is no significant change in the stability derivatives when we vary the cone angles and arch of the ogive. The trend reversal remains at  $h = 0.85$ .

## CONCLUSIONS

Following the above discussion, the concluding remarks are as under:

- Results show that the values of  $C_{mq}$  are maximum at Mach  $M = 5$ , and  $\lambda = 5$ , a constant decrease in the numerical values with the upsurge of Mach  $M = 5$  to 9 and  $\lambda = 5$  to 10. There is a shift of minima towards the downstream, which is advantageous from stability consideration.
- With additional growth in Mach number, the flow parameters do not change despite the rise in Mach values due to the Mach number neutrality.
- When we look at the findings for  $\lambda = -5$  and  $-10$ , a considerable rise in the damping derivatives; however, the impact of cone angle variations on the damping derivatives is marginal except for 20 and 25 degrees. Nevertheless, considerable movement in the center of pressure location is beneficial and enhances the magnitude of damping derivative, resulting in a stable system. The pattern in the variation of the damping derivatives is similar to what was seen for the positive arch.

## REFERENCES

- [1] K. Ghosh, "A New Similitude for Aerofoils in Hypersonic Flow", Proceedings of the 6th Canadian Congress of Applied Mechanics, Vancouver, Canada, May 29-June 3, Pp. 685-686, 1977.
- [2] K. Ghosh, "Hypersonic large deflection similitude for oscillating delta wings", The Aeronautical Journal, Pp. 357-361, 1984.
- [3] S.A. Khan, and A. Crasta, "Oscillating Supersonic delta wings with curved leading Edges", Advanced Studies in Contemporary Mathematics, Vol. 20, No. 3, Pp. 359-372, 2010.
- [4] A. Crasta and S.A. Khan, "Effect of Angle of Incidence on Stability derivatives of a Wing", IET Conference Publications, 2013.

- [5] A. Crasta, S. Pavitra, and S.A. Khan, "Estimation Of Surface Pressure Distribution On A Delta Wing With Curved Leading Edges In Hypersonic/Supersonic Flow," International journal of energy, environment, and Economics, Nova Science publishers inc, Vol. 24, Pp.67-73, 2016.
- [6] A. Shabana, R. Monis, A. Crasta, and S.A. Khan, "Computation of stability derivatives of an oscillating cone for specific heat ratio =1.66," IOP Conf. Series: Materials Science and Engineering, Vol. 370, Pp. 012059, 2018. DOI:10.1088/1757-899X/370/1/012059
- [7] A. Shabana, R. Monis, A. Crasta, and S.A. Khan, "Estimation of stability derivatives in Newtonian Limit for an oscillating cone," IOP Conf. Series: Materials Science and Engineering, Vol. 370, Pp. 012061, 2018. DOI:10.1088/1757-899X/370/1/012061
- [8] A. Shabana, R.S. Monis, A. Crasta, and S.A. Khan, "The Computation of Stiffness Derivative for an Ogive in Hypersonic Flow", International Journal of Mechanical and Production Engineering Research and Development (IJMPERED), Vol. 8, Issue 5, pp. 173-184, 2018. June, ISSN (online): 2249-8001, ISSN (Print): 2249-6890.
- [9] R.S. Monis, A. Shabana, A. Crasta, and S.A. Khan, 2019, "An Effect of sweep angle on roll Damping derivative for a Delta Wing with curved leading edges in unsteady flow", International Journal of Mechanical and Production Engineering Research and Development (IJMPERED), Vol. 9, No. 2, Pp. 361-374, April, ISSN (online): 2249-8001, ISSN (Print): 2249-6890.
- [10] R.S. Monis, A. Shabana, A. Crasta, and S.A. Khan, "Effect of Sweep Angle and a Half Sine Wave on Roll Damping Derivative of a Delta Wing", International Journal of Recent Technology and Engineering (IJRTE) ISSN: 2277-3878, Volume-8, Issue-2S3, Pp. 984-989, 2019. August, DOI : 10.35940/ijrte.B1184.0782S319
- [11] S.A. Khan, A. Aabid, & C, A. S. "CFD Simulation with Analytical and Theoretical Validation of Different Flow Parameters for the Wedge at Supersonic Mach Number", International Journal of Mechanical & Mechatronics Engineering IJMME-IJENS, Vol. 19, No. 01, Pp. 170–177, 2019.
- [12] S.A. Khan, A. Aabid, I. Mokashi, A.A. Al-Robaian, and A.S. Alsagri, "Optimization of Two-dimensional Wedge Flow Field at Supersonic Mach Number", CFD Letters, Vol. 11, No. 5, Pp. 80–97, 2019a.
- [13] W. Asrar, M.F. Baig, S.A. Khan, "Chaos in WAF projectile motion TX wraparound fins, 34th Aerospace Sciences Meeting and Exhibit, 1996.
- [14] W. Asrar, F.M. Baig, S.A. Khan, "Chaos in Wraparound Fin Projectile Motion," Journal of Guidance Control and Dynamics, Vol. 21, No. 2, Pp. 354-356, 1998. DOI: 10.2514/2.7607
- [15] M. Bashir, L. Udayagiri, S.A. Khan, and A. Noor, "Dynamic stability of unguided projectile with 6-DOF trajectory modeling," 2nd International Conference for Convergence in Technology, I2CT 2017, 2017-January, pp. 1002-1009.